Lower hybrid current drive efficiency at high density on Tore Supra

M. Goniche, P. K. Sharma, V. Basiuk, Y. Baranov, C. Castaldo et al.

Citation: AIP Conf. Proc. **1406**, 407 (2011); doi: 10.1063/1.3665003
View online: http://dx.doi.org/10.1063/1.3665003
View Table of Contents: http://proceedings.aip.org/dbt/dbt.jsp?KEY=APCPCS&Volume=1406&Issue=1
Published by the American Institute of Physics.

Lower hybrid current drive efficiency at high density on Tore Supra

M.Goniche, P.K.Sharma[1], V.Basiuk, Y.Baranov[2], C.Castaldo[3], R.Cesario[3], J.Decker, L.Delpech, A.Ekedahl, J.Hillairet, K.Kirov[2], D.Mazon, T.Oosako, Y.Peysson, M.Prou

CEA, IRFM, F-13108 Saint Paul-lez-Durance, France
[1] Institute for Plasma Research, Bhat, Gandhinagar – 382428, India
[2]CCFE, Culham Science Centre, Abingdon, OXON OX14 3DB, UK
[3]Associazione EURATOM / ENEA sulla Fusione, Frascati, Italy

Lower Hybrid waves have shown to have a high current drive (CD) efficiency ($\eta = \overline{n_e} R I_{LH}/P_{LH} \sim 0.3\times10^{20} A.W^{-1}m^{-2}$) suitable for current profile modification [1, 2]. These results were obtained at rather low density ($\overline{n_e} < 3\times10^{19}m^{-3}$) whereas the steady state scenario of ITER requires a density $n_e \approx 7\times10^{19}m^{-3}$. Recent results on C-Mod [3], FTU [4] and JET [5, 6] indicate that CD efficiency could decrease at high density. On C-Mod and FTU, a strong decrease of the fast electron bremsstrahlung in the hard X-ray (HXR) range is measured when the density exceeds $5\times10^{19}m^{-3}$. On JET, the analysis of the contribution of fast electrons to the electron cyclotron emission (ECE) spectrum suggests that the efficiency is reduced for pulses performed with the JET steady state scenario characterized by high density at the pedestal ($\sim3\times10^{19}m^{-3}$) and rather high line-averaged density ($\overline{n_e} \approx 5\times10^{19}m^{-3}$).

On Tore Supra, experiments were carried out with the volume averaged density $\langle n_e \rangle$ in the range of $1.5\text{-}5.3\times10^{19}m^{-3}$ ($\overline{n_e} = 2\text{-}6\times10^{19}m^{-3}$) in deuterium. The plasma is generally leaning on the bottom toroidal pumped limiter (TPL) but a few experiments were carried out with a small outboard limiter (LPA). All the pulses were performed with the same plasma current (1MA) and toroidal field (3.8T). LH power launched from the PAM launcher [7] was 2MW (unless specified) and the main parallel index of the wave N//=1.8 or 1.9. For this set of parameters, the wave gets marginally accessible to the confined plasma when $\langle n_e \rangle = 5\times10^{19}m^{-3}$. Fast electron population is diagnosed from the multi-channel HXR diagnostic [8] and the ECE diagnostic [9].

1) LH power deposition

LH power deposition profiles can be estimated from HXR profiles obtained after Abel inversion of the line-integrated signals provided by the 21 lines of sight of the camera located in the mid-plane. For the whole range of density ($\langle n_e \rangle = 1.5\text{–}5.3\times10^{19}m^{-3}$), the LH deposition is peaked at r/a=0.20 whereas the deposition broadness slightly increases with density between 1.5 and $2.1\times10^{19}m^{-3}$, decreases for higher density and is unchanged for density exceeding $3.5\times10^{19}m^{-3}$ (Fig.1). The LH power deposition was also investigated at lower current I_p=0.6MA. In that case we found a slight increase of the radial location of the maximum of emission from r/a=0.19 to r/a=0.21 when the density increases from $1.5\times10^{19}m^{-3}$ to $2.4\times10^{19}m^{-3}$ when the broadness also slightly increases. In the latter experiments, the LHCD power was modulated between 0.5MW and 2.3MW at 40Hz and the analysis of the electron temperature response in amplitude and phase by the ECE diagnostic provides the LH power deposition. This is true for the central lines of sight of the diagnostic (r/a<0.5) for which the contribution of the fast electrons os negligible. A very good agreement is found with the HXR diagnostic for the low to medium density plasmas.

Radio Frequency Power in Plasmas
AIP Conf. Proc. 1406, 407-410 (2011); doi: 10.1063/1.3665003

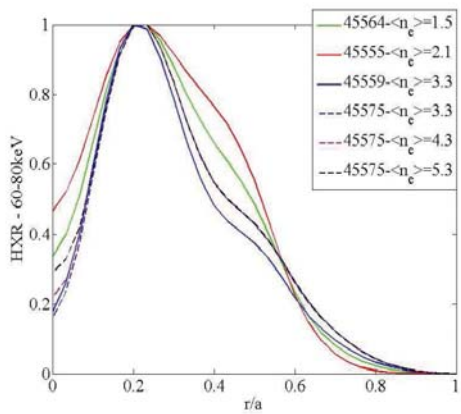

Fig.1. HXR emission (60-80keV) profiles for various plasma densities ($N_{//0}$=1.8)

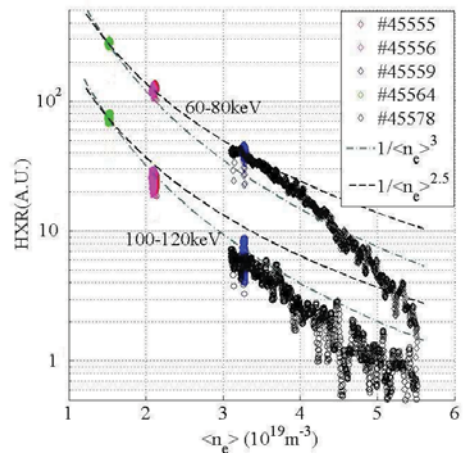

Fig.2. Line integrated HXR emission (central chord) for two energy channels ($N_{//0}$=1.8).

2) Bremsstrahlung and not thermal ECE for high density plasmas.

For the whole range of density, strong decay of the fast electron bremsstrahlung is found with a density dependence very close to $<n_e>^{-2.5}$ in the 60-80keV range and to $<n_e>^{-3.5}$ in the 100-120keV range. For the highest densities ($<n_e> > 4\times10^{19}m^{-3}$), the HXR emission even decays faster (Fig.2). The temperature of the down-shifted ECE radiation from the fast electron tail (T_{tail}) decreases from 11keV to 0.2keV when $<n_e>$ increases from $3.1\times10^{19}m^{-3}$ to $5.3\times10^{19}m^{-3}$. For the highest density, this low temperature is still above the temperature of the thermal plasma estimated to be 0.1keV, 1.5cm inside the LCFS consistently with the low 60-80 and 100-120keV photon counts which are above the noise level. Increasing $N_{//0}$ from 1.8 to 1.9 results in a slight increase of the HXR integrated signal (+10%) at $<n_e>\sim3.5\times10^{19}m^{-3}$ whereas T_{tail} is not significantly changed. The expected highest CD efficiency, scaling as $1/N_{//}^2$, is likely to be compensated by the highest electron temperature for the pulse performed at the highest $N_{//}$.

Reducing the minor radius from 0.72m to 0.66m allows changing the limiter on which the plasma is leaning while minimizing the interaction with the others which are at least 6cm beyond the LCFS. When the plasma is leaning on the LPA, the wetted surface is estimated to be ~0.1m^2 (20 times smaller than that of TPL) and strong recycling occurs. No significant difference could be found for the HXR emission whereas the non thermal emission indicates a lower radiation temperature (-20%) for the LPA configuration. In both cases, the antenna is located 8cm behind the LCFS. The antenna was approached by 4cm to quantify the effect of the width of the scrape-off layer in front of the antenna. It was found a very modest increase of the HXR (T_{rad} resp.) by 10% (15% resp.) whereas the electron temperature of the plasma decreases by 4%. For these two pulses, the plasma density ramps are identical and the magnetic flux consumption can be compared: for density lower than $4\times10^{19}m^{-3}$, the loop voltage, averaged on 3s, is lower by 3% (13mV) for the short scrape-off case, whereas for density higher than $4.8\times10^{19}m^{-3}$, the loop voltage, averaged on 1s, is higher by 5% (40mV). This increase seems related to very high plasma density in front of the antenna and increase of metallic impurity (Fe and Cu) release by up to 50%.

The strongest effect was found when comparing discharges with different minor radius (a_{min}=0.72m and 0.66m), keeping all other parameters constant. For the whole range of density, HXR emission is larger for the small plasma case by a factor ~1.5 in the 60-80keV range and ~1.7 o the 100-120keV range (fig.3). This increase is much larger than that we could expect from an increase of the plasma electron temperature of ~20%. The saturation current of a Langmuir probe embedded in the launcher allows to quantify the fluctuation rate

in the 10-500kHz. For these two cases, the saturation current increases with plasma density identically but the fluctuation rate of this quantity evolves differently. For the small plasma case, the fluctuation rate is almost independent of the core and edge density. For the large plasma case, when the density increases the fluctuation rate is first rather independent of density (and close to that of the small plasma case) and then increases sharply (fig.4). This strong increase is well correlated to the strong decay of HXR emission when the density exceeds ~4 $\times 10^{19} m^{-3}$). In this case, frequency spectra indicate a higher high frequency component [9].

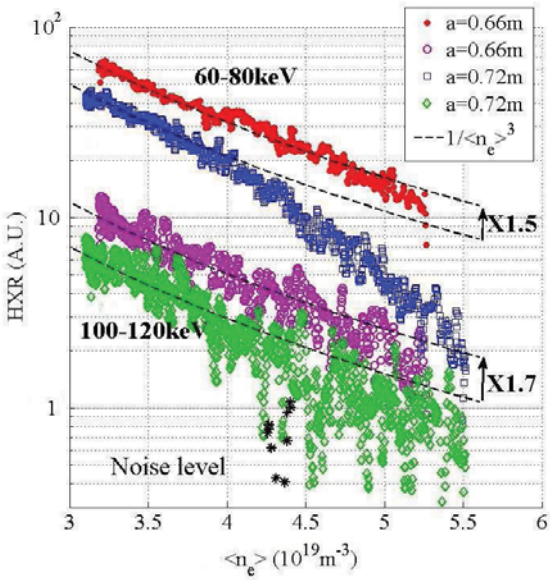

Fig.3. Line- integrated HXR emission for two minor plasma radius for two energy channels. P_{LH}=2MW, $N_{//0}$=1.8.

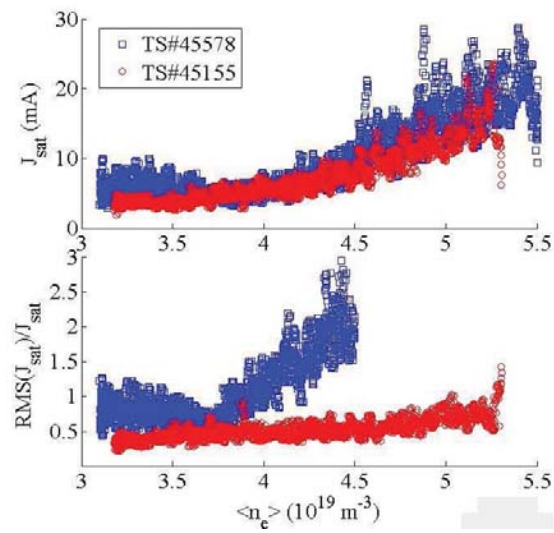

Fig.4. Fluctuation rates the two pulses of figure 3. P_{LH}=2MW, $N_{//0}$=1.8.

3) Modelling of LHCD

The pulses of figure 3 and 4 have been modelled with the CRONOS suite of codes, including C3PO/LUKE for the LHCD part [9]. The full $N_{//}$ spectrum with 6 N// peaks are considered. The rays are launched from 2 poloidal locations. These simulations indicate chaotic behaviour of the launched rays and data (LH current profile, total driven current) exhibit large scattering, typically ±50%. However, some properties can be established. The LH current profile is centred between r/a=0.1 and r/a=0.4 and no evolution is found when the density increases, consistently with the measurement of the HXR profiles. Globally the current drive efficiency ($\eta = \overline{n_e} R I_{LH}/P_{LH}$) decays with density with a general trend which is not far from n_e^{-2}. The decrease is partly due to the decrease of electron temperature from 3keV to 1.6keV at r/a=0.2. The efficiency at $\langle n_e \rangle = 3.5\times10^{19} m^{-3}$ ($\overline{n_e} = 4\times10^{19} m^{-3}$) is found to be $0.62\times10^{19} A.W^{-1}.m^{-2}$ (resp. $0.76\times10^{19} A.W^{-1}.m^{-2}$) for the large (resp. small) minor radius pulses. This value is close to that measured at low current (0.5MA), low density ($\overline{n_e} = 1.4\times10^{19} m^{-3}$) when the current is fully non inductive ($0.57\times10^{19} A.W^{-1}.m^{-2}$).

4) Discussion and conclusion

The strong HXR decay in the full range of density ($1.6\text{-}5.3\times10^{19} m^{-3}$) does not seem inconsistent with the computed LH driven current. However full assessment would require a reconstruction of the line-integrated signals for the different energy channels of the bremsstrahlung diagnostic. It should be mentioned that, as a very crude approximation, the

HXR emission per unit of plasma volume from fast electrons with energy much above the energy of the thermal particles is proportional to the fast electron density n_{fast} and to the density of targets which is $Z_{eff}\times n_e$ where Z_{eff} and n_e are, respectively, the local effective charge and electron density. Introducing the LHCD efficiency, the HXR intensity can be written as $I_{HXR}\sim\eta Z_{eff}P_{LH}E_{fast}^{-1/2}$. Assuming the standard Z_{eff} dependence of η, $I_{HXR}\sim\eta_0[Z_{eff}/(5+Z_{eff})]$ $P_{LH}E_{fast}^{-1/2}$. For $<n_e> > 3\times10^{19}m^{-3}$, line-integrated Z_{eff} varies as $<n_e>^{-1}$ between 1.3 and 2.1. Moreover the photon temperature is quite constant (E_{ph}=30-35keV) for these high density cases. We conclude that the decrease of fast electron bremsstrahlung with density is partly due to the decrease of Z_{eff} which profile is, moreover, likely to peak when density decreases.

For the whole range of density, the decrease of HXR emission is accompanied by a decrease of the electron confinement computed from the kinetic profiles. Normalized to the confinement time given by the Rebut-Lallia-Watkins scaling, the confinement decreases linearly with density from 1.4 to 0.6. This suggests power loss to the thermal electrons. Small plasmas which have higher bremsstrahlung intensity (factor 1.5) have also better confinement of thermal electrons (factor 1.3 for $<n_e> = 3\times10^{19}m^{-3}$). Diamagnetic energy is also higher for small plasmas.

Fluctuation measurements near the LH antenna indicate good correlation with HXR measurements. For standard plasmas (a=0.72m), the fluctuation rate increases sharply when the HXR emission decreases even further than the $<n_e>^{-3}$ scaling ($<n_e> > 4\times10^{19}m^{-3}$) whereas the emission follows this scaling for the smaller plasma case with almost constant fluctuation rate (fig.3 and 4). Similar result to the small plasma case was obtained when standard plasmas are pellets fuelled with the same threshold in density [6].

Modelling with ray tracing coupled to Fokker Planck codes confirm that the rays ($N_{//}$=1.8) are still absorbed for $<n_e>$ $5.2\times10^{19}m^{-3}$ ($n_e(r/a=1)\approx3\times10^{19}m^{-3}$) after a very long path.

[1] Baranov Y. et al. Nucl. Fusion , **36** (1991) 10
[2] Gormezano C. et al., Fusion Sci.Technol. **45**(2004) 1031
[3] Wallace G.M. et al., Phys. Plasmas, **17**, 082508 (2010)
[4] Cesario R. Et al., Nature Commun., **1 ,** 55 (2010)
[5] Kirov K.K. et al., Nucl. Fusion **50** (2010) 075003 (17pp)
[6] Goniche et al., , Plasma Phys. Control. Fusion **52** (2010) 124031 (18pp)
[7] Preynas M. et al., this conference
[8] Peysson Y.et al. , Rev. Sci. Instrum., **70** (1999) 3987-4007
[9] Decker J. et al., this conference
[10] Peysson et al., this conference